Fiber-optic nonlinear endomicroscopy with focus scanning by using shape memory alloy actuation

Yicong Wu,[a] Yuying Zhang,[a] Jiefeng Xi,[a] Ming-Jun Li,[b] and Xingde Li[a]
[a]Johns Hopkins University, Department of Biomedical Engineering, Baltimore, Maryland 21205
[b]Corning Incorporated, Science and Technology Division, SP-AR-02-2, Corning, New York 14831

Abstract. A miniature fiber optic endomicroscope with built-in dynamic focus scanning capability is developed for the first time for 3-D two-photon fluorescence (TPF) imaging of biological samples. Fast 2-D lateral beam scanning is realized by resonantly vibrating a double-clad fiber cantilever with a tubular piezoactuator. Slow axial scanning is achieved by moving the distal end of the imaging probe with an extremely compact electrically driven shape memory alloy (SMA). The 10-mm-long SMA allows 150-μm contractions with a driving voltage varying only from 50 to 100 mV. The response of the SMA contraction with the applied voltage is nonlinear, but repeatable and can be accurately calibrated. Depth-resolved imaging of acriflavine-stained biological tissues and unstained white paper with the endomicroscope is performed, and the results demonstrate the feasibility of 3-D nonlinear optical imaging with the SMA-based scanning fiber-optic endomicroscope. [DOI: 10.1117/1.3523234]

Keywords: two-photon fluorescence; endomicroscope; focus scanning; shape memory alloy.

Paper 10528LR received Sep. 28, 2010; revised manuscript received Nov. 3, 2010; accepted for publication Nov. 9, 2010; published online Dec. 30, 2010.

1 Introduction

Two-photon fluorescence (TPF) endomicroscopy is an emerging technology that has the ability to potentially assess 3-D structural and biochemical information of biological tissues with miniaturized scanning fiber optic probes.[1,2] This technology is critical for translating powerful nonlinear optical sectioning microscopy[3,4] to clinical practice, and can be potentially integrated with a standard clinical endoscopy procedure for diagnosis *in situ* and real-time guidance of biopsy. Various 2-D scanning mechanisms in a small footprint have been demonstrated, including the use of piezo-based actuators to swing the imaging fiber cantilever, or microelectromechanical system (MEMS)-based micromirrors to scan the imaging beam.[1,2,5–7] To achieve accurate depth scanning and maintain a small footprint, a built-in mechanism has to be implemented at the distal end (e.g., for changing the focal plane), which faces many challenges, including system miniaturization, reduction in the actuation voltage, and improvement on focus scanning accuracy and repeatability over a sufficient range.[8,9] In this study, we report the use of an electrically driven shape memory alloy (SMA) to achieve slow axial scanning at the distal end by moving the distal end of endomicroscope (including the miniature focusing optics and piezoelectric transducer (PZT)-based beam scanner). By integrating the SMA-based depth scan with a 2-D fiber optic resonant scanner, real-time 3-D two-photon fluorescence imaging becomes feasible for the first time with a compact fiber optic endomicroscope, which is demonstrated by imaging various samples including biological samples.

Address all correspondence to Xingde Li, Johns Hopkins University, Dept. of Biomedical Engineering, Rm. 731B, Ross Building, 720 Rutland Ave., Baltimore, MD 21205. Tel: 410-955-0075; Fax: 410-502-9814; E-mail: xingde@jhu.edu.

2 Methods and System

Shape memory alloy (SMA) is a special type of metal that can remember its original cold-forged shape and return to this shape after being deformed by applying heat.[10,11] This material has shown promising applications in medical devices over conventional actuators such as hydraulic, pneumatic, and motor-based systems due to its ultralight weight, compact size, and relatively simple operation.[12,13] SMA can be fabricated as a small wire that can contract up to 5% of its original length when it is heated above room temperature. With advances in manufacturing technologies, it becomes possible for SMA to operate reliably over tens of millions of cycles. In this study, we employed an SMA wire made of nickel-titanium. The SMA wire had an extraordinary ability to accommodate large strains with a pull force of 80 g while maintaining an ultrasmall diameter (0.003 in.). The heating and corresponding temperature changes were achieved by applying an electrical current through the thin wire of internal resistance of 5 ohms/in. In addition, the SMA had shown physiological and chemical compatibility with the human body.[14,15]

Figures 1(a) and 1(b) show the schematic and photograph of the distal end of the fiber optic endomicroscope integrated with a SMA wire (for focus or depth scanning), along with a fiber optic resonant scanner (for lateral beam scanning). Mechanically, the endomicroscope probe was composed of three parts: 1. tube 1, which encases a fiber optic scanner and the imaging optics; 2. tube 2, which is hollow and fixed to the proximal end; and 3. an SMA wire and compressed spring that connect the two tubes. A short extruded portion of tube 1 can freely slide within tube 2 once the SMA contracts or expands. The imaging optics within tube 1 is similar to what was reported previously.[5] Basically, it consisted of a double-clad fiber (DCF) with a 5.1-μm-diam core for single-mode femtosecond laser delivery and a 135-μm-diam inner clad for multimode nonlinear optical signals collection, a miniature tubular PZT for resonantly sweeping the DCF cantilever in a spiral pattern, and a gradient-index (GRIN) lens as the focusing unit with a magnification of 0.5 from the DCF tip to the sample. The overall diameter for both tube 1 and tube 2 was 2.4 mm.

When an electrical current is applied to the SMA wire, it contracts through Joule heating and compresses the spring, consequently pulling tube 1 (along with the imaging optics) toward tube 2. When the Joule heating current decreases or stops, the SMA relaxes and the spring pushes the imaging tube back to its original position. Figure 2(a) shows the travel distance of tube

1083-3668/2010/15(6)/060506/3/$25.00

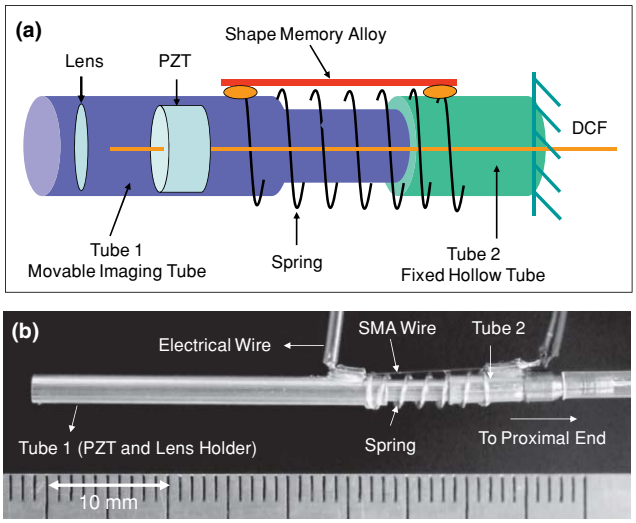

Fig. 1 (a) Schematic and (b) photograph of the distal end of the scanning fiber optic two-photon fluorescence endomicroscope capable of dynamic focus scanning. One side of the SMA wires and spring was mounted on a movable imaging tube (tube 1), which housed the resonant fiber scanner and miniature lens, while the other side was mounted on a fixed hollow tube (tube 2). The contraction and extension of the SMA wires and spring allow the short extruded portion of tube 1 to slide within tube 2 for depth scanning. DCF: double-clad fiber; SMA: shape memory alloy; PZT: tubular piezoelectric actuator. (Color online only.)

1 as a function of the SMA drive voltage during the courses of SMA/spring contraction and expansion. The video in Fig. 2(b) shows the continuous motion of tube 1 when the SMA wire was driven with a triangle waveform at a frequency of 0.25 Hz. As can be seen, a ~150-μm axial scan can be achieved with an extremely low drive voltage (i.e., less than 100 mV). As for the depth scanning speed, it took about 1 s to achieve full contraction, whereas it took about 1.3 s to expand back to its original length after shutting down the drive voltage. Although the response of the SMA contraction/expansion with the applied voltage was nonlinear and exhibited hysteresis, tube 1 translation (i.e., depth scanning) was repeatable and the nonlinearity could be calibrated to achieve a depth scanning accuracy better than 10 μm. Additionally, there was a small lateral shift (less than 5 μm over the total 150-μm depth scan) on the axial trajectory due to the one-sided SMA actuation, which can be potentially reduced by employing multiple SMA wires.

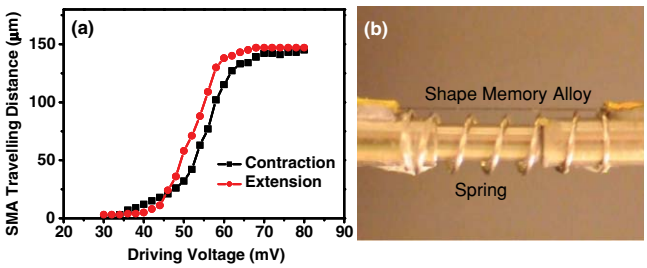

Fig. 2 (a) Traveling distance of the imaging tube (tube 1) as a function of the SMA drive voltage during the SMA contraction and expansion phase. (b) A video showing the continuous motion of tube 1 when the SMA is electrically driven with a triangle waveform. Upper portion: full view; lower portion: zoomed view. (QuickTime, 5MB) [URL: http://dx.doi.org/10.1117/1.3523234.1]

The details of the endomicroscopy imaging system were described elsewhere.[5] In essence, a home-built Ti:sapphire laser prechirped by a single photonic bandgap fiber was coupled into the endomicroscope through the DCF core for effective excitation. The nonlinear optical signals from the samples were collected by both the core and inner clad of the DCF and directed to a photomultiplier tube (PMT). The fiber optic resonant scanner created a scanning diameter of 150 μm on the sample. Depth-resolved imaging was synchronized with the SMA contraction driven by a step-wise triangle waveform. Each image at each step was averaged over five frames with a total sampling time of ~1.5 s per averaged image.

3 Results and Discussions

Figure 3 shows representative depth-resolved two-photon fluorescence intensities and images acquired from *ex-vivo* pig esophageal tissue. Each intensity value is the averaged intensity over the frame at each given depth, while the images are normalized to the maximal intensity of each image. The tissue was stained with 0.01% acriflavine (a dye that predominantly stains nuclei) for one hour, followed by a wash in phosphate-buffered saline (PBS) three times to remove excessive acriflavine molecules. Figure 3(a) shows the TPF intensities as a function of the SMA drive voltage during the course of contraction and expansion. It is noted that the TPF intensities exhibit different voltage dependence during SMA contraction and expansion, indicating the hysteresis effect of the SMA. After calibrating the drive voltage against the scanning depth based on Fig. 2(a), TPF intensities versus the sampling depth are shown in Fig. 3(b). For comparison, Fig. 3(b) also shows the depth-resolved TPF intensities measured with a precision translation stage (of 0.1-μm accuracy) by moving the entire endomicroscope probe with an axial step of 10 μm. In the figure, the 0-μm depth is supposed to be the tissue surface where the fluorescence intensity is maximal, and the positive values along the depth axis refer to imaging within the tissue. After depth

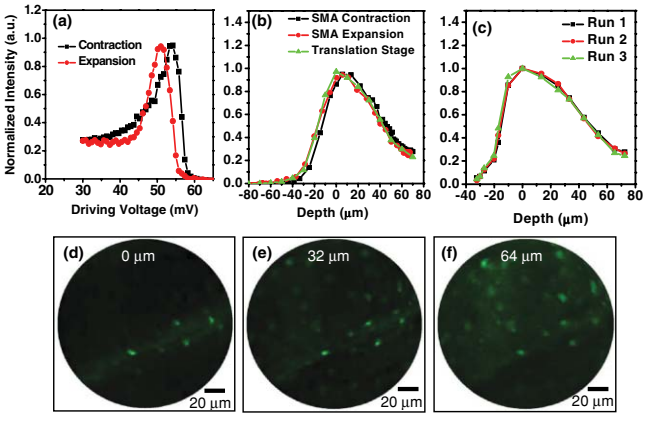

Fig. 3 (a), (b), and (c) Representative depth-resolved TPF intensities and (d), (e), and (f) images recorded from acriflavine-stained pig esophagus: (a) TPF intensities as a function of SMA drive voltage during the course of contraction and expansion; (b) depth-resolved TPF intensities obtained with the SMA and a precision translation stage; and (c) three randomly selected depth-dependent TPF intensity profiles during multiple SMA contractions. (d), (e), and (f) Typical TPF images recorded at depths of (d) 0, (e) 32, and (f) 64 μm.

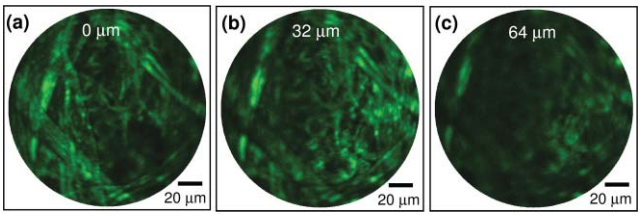

Fig. 4 Typical depth-resolved TPF images acquired from a piece of unstained white paper at depths of (a) 0, (b) 32, and (c) 64 μm. The images were obtained during SMA contraction. (Color online.)

calibration, the depth-resolved TPF intensities during the courses of SMA contraction and expansion overlap nicely, and are also in good agreement with the intensity profile measured by translating the entire probe with a precision translation stage. It suggests that the nonlinear response of the SMA as a function of drive voltage can be accurately calibrated to represent the scanning depth. Figure 3(c) shows the depth-resolved TPF intensities from the same sample/site during the course of SMA contraction. The nice overlap of the three randomly selected TPF depth-dependent profiles suggests an excellent repeatability of the SMA as a depth scanner with a measured accuracy better than 10 μm.

Figures 3(d), 3(e), and 3(f) show some representative TPF images at depths of 0, 32, and 64 μm within the tissue sample, respectively. The epithelial cellular nuclei can be easily identified at all depths, and as expected in stratified squamous epithelium, the cell density varies with depth. Overall, these endomicroscopic TPF intensities and images as a function of depth demonstrate that the extremely thin SMA actuator along with a spring can effectively perform depth scanning in a compact endomicroscope probe for depth-resolved TPF imaging.

Figures 4(a), 4(b), and 4(c) show another example of the depth-resolved TPF imaging achieved with a SMA-based focus scanning mechanism. The sample was a piece of unstained white paper and depths were calibrated at 0, 32, and 64 μm, respectively. As shown, different fiber structures can be clearly resolved at different depths, with the fiber diameter varying from a few microns to around 20 μm. Again, these imaging results demonstrate the feasibility of the SMA-based scanning mechanism for enabling depth scanning on an endomicroscope of a small form factor. Thus, 3-D nonlinear optical endomicroscopy imaging becomes possible.

4 Conclusions

In summary, a flexible fiber optic endomicroscope capable of dynamic depth scanning is developed for 3-D nonlinear optical imaging of biological samples. Depth scanning is achieved with high accuracy and good repeatability by using ultrathin SMA wires that require an extremely low drive voltage. It is expected that the performance of the endomicroscope can be further improved by moving only the focusing lens (as opposed to both the lens and the fiber optic scanner) and by developing a drive waveform to produce linear depth scanning.

Acknowledgments

This research was supported in part by the National Institutes of Health (CA120480, CA116442, and EB007636) and the National Science Foundation (Career Award, Li).

References

1. M. T. Myaing, D. J. MacDonald, and X. D. Li, "Fiber-optic scanning two-photon fluorescence endoscope," *Opt. Lett.* **31**, 1076–1078 (2006).
2. L. Fu, A. Jain, C. Cranfield, H. K. Xie, and M. Gu, "Three-dimensional nonlinear optical endoscopy," *J. Biomed. Opt.* **12**(4), 040501 (2007).
3. W. R. Zipfel, R. M. Williams, R. Christie, A. Y. Nikitin, B. T. Hyman, and W. W. Webb, "Live tissue intrinsic emission microscopy using multiphoton-excited native fluorescence and second harmonic generation," *Proc. Natl. Acad. Sci. USA* **100**, 7075–7080 (2003).
4. M. C. Skala, J. M. Squirrell, K. M. Vrotsos, V. C. Eickhoff, A. Gendron-Fitzpatrick, K. W. Eliceiri, and N. Ramanujam, "Multiphoton microscopy of endogenous fluorescence differentiates normal, precancerous, and cancerous squamous epithelial tissues," *Cancer Res.* **65**, 1180–1186 (2005).
5. Y. C. Wu, Y. X. Leng, J. F. Xi, and X. D. Li, "Scanning all-fiber-optic endomicroscopy system for 3D nonlinear optical imaging of biological tissues," *Opt. Express* **17**, 7907–7915 (2009).
6. W. Piyawattanametha, E. D. Cocker, L. D. Burns, R. P. J. Barretto, J. C. Jung, H. Ra, O. Solgaard, and M. J. Schnitzer, "In vivo brain imaging using a portable 2.9 g two-photon microscope based on a microelectromechanical systems scanning mirror," *Opt. Lett.* **34**, 2309–2311 (2009).
7. Y. C. Wu, J. F. Xi, M. J. Cobb, and X. D. Li, "Scanning fiber-optic nonlinear endomicroscopy with miniature aspherical compound lens and multimode fiber collector," *Opt. Lett.* **34**, 953–955 (2009).
8. A. R. Rouse, A. Kano, J. A. Udovich, S. M. Kroto, and A. F. Gmitro, "Design and demonstration of a miniature catheter for a confocal microendoscope," *Appl. Opt.* **43**, 5763–5771 (2004).
9. H. Makhlouf, A. F. Gmitro, A. A. Tanbakuchi, J. A. Udovich, and A. R. Rouse, "Multispectral confocal microendoscope for in vivo and in situ imaging," *J. Biomed. Opt.* **13**, 044016 (2008).
10. C. A. Rogers, "Intelligent materials," *Sci. Am.* **273**, 154–157 (1995).
11. K. Otsuka and X. B. Ren, "Recent developments in the research of shape memory alloys," *Intermetal.* **7**, 511–528 (1999).
12. T. Duerig, A. Pelton, and D. Stockel, "An overview of nitinol medical applications," *Mat. Sci. Eng. Struct.* **273**, 149–160 (1999).
13. C. Mavroidis, "Development of advanced actuators using shape memory alloys and electrorheological fluids," *Res. Nondestruct. Eval.* **14**, 1–32 (2002).
14. J. Ryhanen, M. Kallioinen, J. Tuukkanen, J. Junila, E. Niemela, P. Sandvik, and W. Serlo, "In vivo biocompatibility evaluation of nickel-titanium shape memory metal alloy: Muscle and perineural tissue responses and encapsule membrane thickness," *J. Biomed. Mater. Res.* **41**, 481–488 (1998).
15. N. B. Morgan, "Medical shape memory alloy applications — the market and its products," *Mat. Sci. Eng. Struct.* **378**, 16–23 (2004).